Hall Effect of Spin-Chirality Origin in a Triangular-Lattice Helimagnet $Fe_{1.3}Sb$

Y. Shiomi,[1] M. Mochizuki,[1] Y. Kaneko,[2] and Y. Tokura[1,2,3]

[1]*Department of Applied Physics, University of Tokyo, Tokyo 113-8656, Japan*
[2]*Multiferroics Project, ERATO, Japan Science and Technology Agency (JST), Tokyo 113-8656, Japan*
[3]*Cross-Correlated materials Research Group (CMRG)/ Correlated Electron Research Group (CERG), ASI, RIKEN, Wako 351-0198, Japan*

(Received 9 September 2011; published 30 January 2012)

We report on a topological Hall effect possibly induced by scalar spin chirality in a quasi-two-dimensional helimagnet $Fe_{1+\delta}Sb$. In the low-temperature region where the spins on interstitial-Fe (concentration $\delta \sim 0.3$) intervening the 120° spin-ordered triangular planes tend to freeze, a nontrivial component of Hall resistivity with opposite sign of the conventional anomalous Hall term is observed under magnetic field applied perpendicular to the triangular-lattice plane. The observed unconventional Hall effect is ascribed to the scalar spin chirality arising from the heptamer spin clusters around the interstitial-Fe sites, which can be induced by the spin modulation by the Dzyaloshinsky-Moriya interaction.

DOI: 10.1103/PhysRevLett.108.056601 PACS numbers: 72.15.−v, 72.20.My, 75.25.−j, 75.47.−m

The interplay between electron transport and magnetism has been a central subject of condensed-matter physics. The Hall effect (HE) in ferromagnets as one such example is known to have two contributions: one is the ordinary Hall effect induced by Lorentz force, which is proportional to magnetic field (H), and the other is the anomalous Hall effect (AHE), which arises usually from the spin-orbit interaction and is driven by the magnetization (M). While AHE was discovered more than a century ago, the theoretical elucidation has been a controversial issue [1]. Recently, a connection to Berry phase of Bloch electrons in $\boldsymbol{k}$ space was proposed as the origin of intrinsic AHE [2,3], which has turned out to be a nonperturbative extension of Kaplus-Luttinger theory [4], and to successfully explain the *intrinsic* AHE observed in some of ferromagnets, such as Fe [5] and $SrRuO_3$ [6]. In this theory, the energy gap induced by the spin-orbit interaction at the band-crossing point acts as a fictitious magnetic field (Berry-phase curvature) in $\boldsymbol{k}$ space and hence ensures the nondissipative nature of anomalous Hall current.

While the anomalous Hall resistivity is usually proportional to M, a counter example has recently been found in the case of a ferromagnetic pyrochlore $Nd_2Mo_2O_7$ [7]; the magnitude of the Hall resistivity increases with decreasing temperature (T) and the H dependence seems not to be related straightforwardly to that of M. This HE has been interpreted as originating from the noncoplanar configuration of Mo spins. The scalar spin chirality [$\chi_{ijk} = \boldsymbol{S}_i \cdot (\boldsymbol{S}_j \times \boldsymbol{S}_k)$] associated with the noncoplanar spin-configuration endows the conduction electron with the Berry phase in $\boldsymbol{k}$ space, just as the relativistic spin-orbit interaction does. A similar unconventional HE was also reported in another pyrochlore $Pr_2Ir_2O_7$ [8].

Although the noncoplanar spin configuration is realized in helical magnets under applied H, the HE of the scalar-spin-chirality origin is usually not observed because the total scalar spin chirality summed over the whole lattice sites often becomes zero [9]. In the case of the triangular lattice with three-sublattice spin order (e.g., 120°-spin structure), the whole scalar spin chirality cancels out and the contribution to HE is not expected [13,14]. Recently, however, in a triangular-lattice antiferromagnet $PdCrO_2$ where Cr^{3+} spins order with a 120°-structure below $T_N = 37$ K, an unconventional HE was observed under H applied parallel to the c axis below $T^* \sim 20$ K that is noticeably lower than T_N [15]. It was speculated in [15] that the spin structure would change so as to have a finite scalar spin chirality below T^* under H applied parallel to the spin-spiral plane, although such a subtle spin-structural modification could not be proved. In this Letter, we report on a more explicit case of the spin-chirality induced HE on the triangular-lattice magnet $Fe_{1+\delta}Sb$, in which we could identify that Dzyaloshinsky-Moriya (DM) interaction modifies the spin structure in the spin clusters associated with the interstitial-Fe spins to generate the net scalar spin chirality. The DM-interaction mediated topological Hall effect (THE) as proposed here may be found in many of triangular-lattice magnets with modified 120°-spin structures.

The crystal structure of $Fe_{1+\delta}Sb$ (NiAs-type) is depicted in Fig. 1(c). Fe and Sb triangular nets are alternately stacked along the c axis, while hosting the interstitial-Fe [Fe(i)] atoms (content δ). The dotted circles in Fig. 1(c) indicate the possible positions which can be randomly occupied by the Fe(i) atoms; these positions correspond to the apex connecting the upper and lower adjacent-lattice Fe triads. $Fe_{1+\delta}Sb$ is always off-stoichiometric ($\delta \neq 0$) and is known to be stabilized for $0.08 < \delta < 0.35$ [16]. Spins of lattice-Fe [Fe(l)] order in a 120°-spin structure within the c plane and ferromagnetically along the c axis

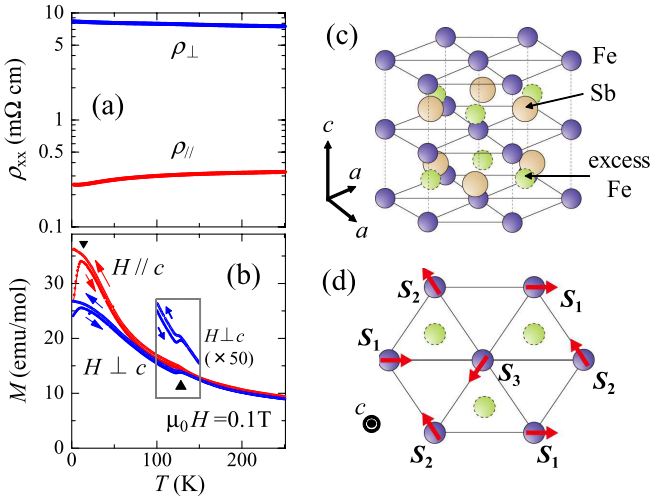

FIG. 1 (color online). (a) Temperature dependence of the in-plane and out-of-plane resistivities, $\rho_\parallel$ and $\rho_\perp$, for $Fe_{1.3}Sb$. (b) T dependence of the magnetization (M) in external magnetic-field (H) parallel or perpendicular to the c axis. Two triangles indicate the ordering temperatures of the in-plane Fe(l) spins (T_N) and the interstitial-Fe(i) spins, respectively. The inset shows the magnified M-T curve around T_N in $H \perp c$. (c) Schematic view of the crystal structure of $Fe_{1+\delta}Sb$. Fe(i) atoms, whose concentration is δ, randomly occupy the sites shown by dotted circles. (d) Top view of the Fe(l) and Fe(i) sites where the (red) arrows indicate the directions of the Fe(l) spins in the 120°-spin structure below T_N.

below T_N [Fig. 1(d)], as determined by the neutron diffraction measurement for $Fe_{1.14}Sb$ [17]. The T_N value obtained from the Mössbauer spectroscopy and susceptibility data decreases from 200 to 50 K with increasing Fe(i) content δ [16]. Spins of Fe(i) do not order at T_N but freeze in the much lower-T region than T_N with the thermal hysteresis in M-T curve [see Fig. 1(b)] [18]. According to the powder neutron diffraction measurement [17], the 120°-spin structure of the Fe(l) spins is still retained in such a low-T region independently of the spin-glass transition of the Fe(i) spins. It is anticipated that the long range 120°-spin order and the spin-glass (mictoglass) state around Fe(i) coexist at the lowest T [18]. Although the magnetic properties have been intensively investigated for $Fe_{1+\delta}Sb$ as described above, little attention has been paid to the transport properties. The development of the local magnetic order on Fe(i) sites is expected to affect the net scalar spin chirality of the system which would be totally canceled out in the 120°-spin structure without Fe(i). We show here that the topological Hall resistivity as induced by the scalar spin chirality is observed in external H applied parallel to the c axis in the low-T region where the chiral magnetic clusters are built up around the Fe(i) sites.

Single crystals of $Fe_{1.3}Sb$ ($\delta = 0.3$) were grown by a Bridgman method, following the procedure described in the literature [17]. The T and H dependences of M were measured by SQUID and extraction-type magnetometers. The Hall resistivity and magnetoresistance were measured within the c plane under H applied parallel to the c axis.

Figure 1(a) shows the T dependence of resistivity measured within and out of the c plane ($\rho_\parallel$ and $\rho_\perp$ respectively). $\rho_\parallel$ slightly decreases with decreasing T, but the residual resistance ratio to the room temperature value is less than 2, suggesting the appreciable effect of disorder by randomly occupying Fe(i). On the other hand, $\rho_\perp$ is 1 order of magnitude larger than $\rho_\parallel$ and slightly increases with decreasing T, indicating the quasi-two-dimensional transport characteristic of the layered lattice structure shown in Fig. 1(c). We show in Fig. 1(b) the T dependence of M measured in H parallel or perpendicular to the c axis. A transition is observed around 130 K, below which Fe(l) spins order in the in-plane 120° spin structure [Fig. 1(d)] [19]. According to the previous study [16], the T_N value corresponds to that of $\delta \sim 0.25$, which is slightly smaller than the nominal value ($\delta \sim 0.3$) in the present crystal. The decrease of M upon T_N in $H \perp c$ is larger than that in $H \| c$. The observed anisotropy is consistent with the magnetic transition to the in-plane 120°-spin order. Since the Fe(i) spins do not order magnetically at T_N, the Curie-like increase of M persists below T_N as observed. Around 10 K, M shows the maximum accompanying the large thermal hysteresis both for $H \| c$ and $H \perp c$. In the present sample, the spin-glass transition relevant to the Fe(i) spins seems to occur around 10 K, which is lower than the value reported in literature (~ 30 K) [17,18].

In Fig. 2(a), we show the magnetoresistance below 90 K. The magnetoresistance is as small as 2% even at 2 K and 14 T. Figure 2(b) shows the $H(\| c)$ dependence of M at several temperatures. The slope of M-H curve increases with decreasing T, but M does not saturate up to 14 T even

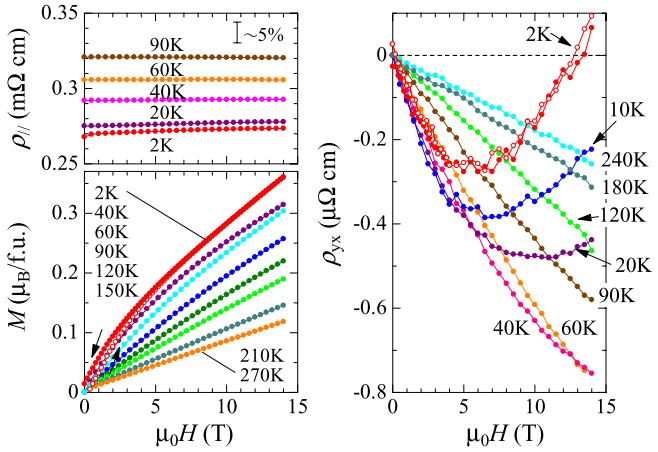

FIG. 2 (color online). Magnetic-field (H) dependence of (a) the in-plane resistivity ($\rho_\parallel$), (b) the magnetization (M), and (c) the Hall resistivity ρ_{yx} under $H \| c$ at several temperatures. Small hysteresis is observed in M and ρ_{yx} at 2 K, as seen as the difference between closed (H-decreasing run) and open (H-increasing run) circles, while hardly discernible in ρ_{yx} above 4 T within the experimental accuracy.

at 2 K; the M at 14 T is about $0.35\mu_B$/f.u., which is far smaller than the full moment value ($\sim 0.9\mu_B$/f.u.) of Fe determined by neutron diffraction measurement [17]. Since the magnetization of Fe(l) (M^l) would not change largely below T_N, the increase of M below T_N should be attributed to the increase in the magnetization of Fe(i) (M^i). For the latter use in the analysis of the Hall resistivity, we estimated the M^l value (assumed to be T independent [20]) by $M^l = \chi^l H$, where the T-independent susceptibility for Fe(l) spins (χ^l) is obtained by the subtraction of the Fe(i) component $\propto 1/(T + T_0)$ from M below T_N in Fig. 1(b). (Here, the fitted Curie-Weiss temperature T_0 is close to $T_g \sim 10$ K.) Thus, the obtained M^l value below T_N based on this assumption is H-linear by definition, and reaches, for example, $0.17\mu_B$/f.u. at 14 T. The observed nonlinear H dependence of M in the low-T region is ascribed to M^i ($\equiv M - M^l$ at every temperature below 120 K). At 2 K, the hysteresis is observed in the M-H curve up to around 5 T, perhaps reflecting the freezing of Fe(i) spins or mictoglass state.

Figure 2(c) shows the Hall resistivity (ρ_{yx}) measured in $H \| c$. ρ_{yx} is negative and almost linear with H above 60 K. The roughly estimated carrier density ($\equiv -1/R_0 e$, where R_0 is normal Hall coefficient) and mobility ($\equiv |R_0|/\rho_\parallel$) above T_N are 1.2×10^{23}/cm^3 and 0.16 cm^2/V s, respectively. Since the magnitude of ρ_{yx} increases with decreasing T in proportional to M, the contribution from the anomalous Hall effect (AHE) as induced by the spin-orbit interaction seems to be dominant below T_N. Below 40 K, ρ_{yx} shows an almost linear H-dependence in the low-H region, but tends to curve positively in the high-H region. Below 20 K, ρ_{yx} increases toward a positive direction in high-H region, and at 2 K shows even a sign-reversal around 13 T, while the magnetoresistance remains as small as a few percent. Judging from the T region in which the anomaly takes place, the order of the Fe(i) spins affects the AHE, whereas no distinct change in the H dependence of M nor $\rho_\parallel$ is observed.

The Hall effect in a magnet is generally described by the empirical formula $\rho_{yx} = R_0(\mu_0 H) + R_s M$, where R_0 and R_s are normal and anomalous Hall coefficients, respectively. For the present material, the contributions from the moments of Fe(l) and Fe(i) should be distinguished, i.e. $\rho_{yx} = R_0(\mu_0 H) + R_s^i M^i + R_s^l M^l$ [R_s^i and R_s^l are R_s for Fe(i) and Fe(l), respectively.] As shown in Figs. 3(a)–3(d), we can fit nicely the experimental data above 40 K using this relation with constant values of R_0, R_s^l, and R_s^i. The obtained values of R_0, R_s^l, and R_s^i are -4.9×10^{-9} Ωcm/T, -1.07×10^{-6} Ωcm/(μ_B/f.u.), and -3.59×10^{-6} Ωcm/(μ_B/f.u.), respectively. The good agreement between ρ_{yx} and the fitting curve with use of these parameters above 40 K [Figs. 3(a)–3(d)] indicates that the Hall effect in the triangular lattice with an in-plane 120°-spin order can be understood within the framework of the conventional AHE. Below 30 K, by contrast, ρ_{yx}

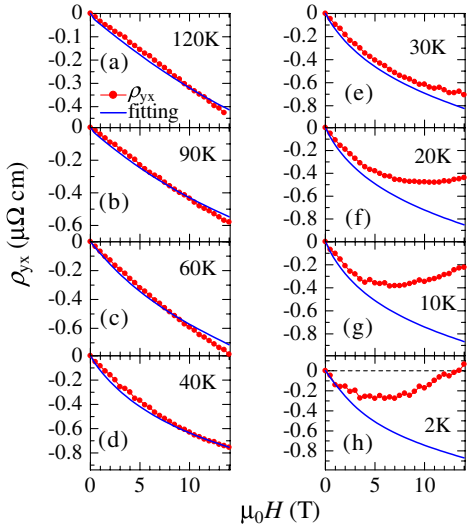

FIG. 3 (color online). (a)–(h) Fitting (solid lines) of the Hall resistivity ρ_{yx} with the relation of $\rho_{yx} = R_0(\mu_0 H) + R_s^i M^i + R_s^l M^l$ below 120 K. Fitting parameters R_0, R_s^i, and R_s^l are assumed to be T independent (see text).

deviates from the fitting curve as shown in Figs. 3(e)–3(h). (At 2 K, we used the average values of M^i (and also ρ_{yx} though negligible) in the hysteresis region for the fitting.) To explain such a large deviation from the conventional fit, one may consider the possibility that the R_s^i value changes with the ordering of the Fe(i) spins around 10 K. However, a dramatic change of R_s^i, including a sign-reversal in H and steep H and T dependences, would be necessary for the explanation of the H dependence of ρ_{yx}; this is highly unlikely. Moreover, R_0 and R_s^l show negative signs above 40 K and these values could be hardly changed by the ordering of the Fe(i) spins. It was confirmed that the different estimation of M^l and M^i least affects the emergent deviation below 30 K, although does slightly the accuracy of the fitting curve above 40 K. Thus, the difference between ρ_{yx} and the fitting curve below 30 K is not explained by the conventional formula and regarded as an unconventional term, which we assign here to the spin-chirality mechanism.

We estimate the chirality-driven ρ_{yx} (ρ_{yx}^χ) as the deviation from the conventional normal and anomalous terms (see Fig. 3) and plot its H dependence below 40 K in Fig. 4(a). ρ_{yx}^χ at 14 T is almost zero at 40 K, but below 30 K increases with decreasing T, as shown in the inset to Fig. 4(a). The onset T for the H (14 T)-induced spin chirality is tangibly higher than the transition T of the Fe (i) spins (~ 10 K), which indicates the spin-glass state is not directly related with the spin chiraliy mechanism. At 2 K, $\sigma_{xy}^\chi = \rho_{yx}^\chi/\rho_\parallel^2$ is $\sim 15\ \Omega^{-1}$ cm $-$ 1 at 14 T. This value is as large as σ_{xy}^χ observed in $Nd_2Mo_2O_7$, in which the scalar spin chirality plays a dominant role due to the tilting ($\sim 4°$) of the Mo spins from the ferromagnetic alignment

[7]. The H dependence of ρ_{yx}^{χ} is approximately linear or slightly superlinear.

In the relatively high-T region below T_N, the Fe(i) spins are almost disordered due to thermal agitation, and the spin order occurs only as the in-plane 120°-spin structure on the Fe(l) triangular lattices as shown in Fig. 1(d). In this situation, the net scalar spin chirality should cancel out in $\boldsymbol{k}$ space as suggested theoretically [13,14], and, thus, no additional Hall effect is expected, being consistent with our observation. On the other hand, in the low-T region where the Fe(i) spins tend to be polarized by external H, there appear some heptamer spin-clusters in which one Fe(i) spin couples to two Fe(l)-triangles with 120°-spin orders located above and below the Fe(i). Because of the alternate stacking of Fe(i) and Sb atoms, there are two kinds of the heptamer clusters with the equal population, A and B, as illustrated in Fig. 4(b). The total scalar spin chirality χ_A (χ_B) for the heptamer cluster A (B) can be calculated as a sum of vectors normal to the respective triangular faces as exemplified by (green) open arrows, whose lengths are χ_{ijk}. When only the symmetric exchange ($J_{ij}\boldsymbol{S}_i \cdot \boldsymbol{S}_j$) works among the Fe spins, the relation $\boldsymbol{S}_m = \boldsymbol{S}'_m = \tilde{\boldsymbol{S}}_m = \tilde{\boldsymbol{S}}'_m$ holds for $m = 1$, 2, and 3 even under $H \parallel c$. Consequently, χ_A coincides with $-\chi_B$, both of which are given by $(2/3)(\chi_{124} + \chi_{234} + \chi_{314}) + 2\chi_{123}$. This is because the cluster B is a mirror image of the cluster A, and each face of the heptamer gives an opposite contribution between A and B. For example, each of the basal and top Fe (l) triads gives χ_{123} for the cluster A, while $-\chi_{123}$ for the cluster B. The perfect cancellation of χ_A and χ_B indicates that we need more ingredients to account for the observed topological Hall effect (THE).

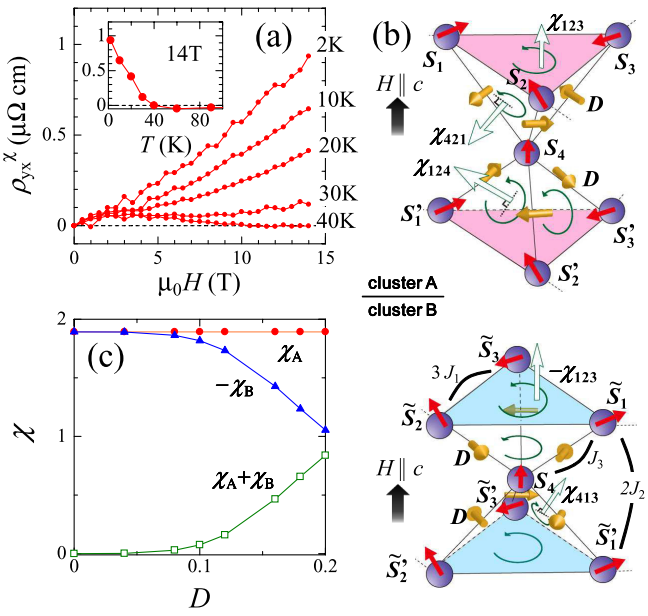

FIG. 4 (color online). (a) Magnetic-field (H) dependence of the chirality-driven Hall resistivity, ρ_{yx}^{χ}, estimated from Fig. 3. Inset shows temperature (T) dependence of ρ_{yx}^{χ} at 14 T. (b) Schematic views of two types of the heptamer spin clusters, A and B, consisting of one Fe(i) spin and two Fe(l)-spin triads above and below it under $H \| c$ at low temperatures. Here the Fe (i) spins are assumed to be well H polarized. Vectors normal to the faces as described by (green) open arrows denote directions of the scalar spin chirality from the respective triangle faces of the heptamer. The (yellow) arrows indicate directions of the DM vectors $\boldsymbol{D}_{ij}$ on the nearest-neighbor Fe(l)-Fe(i) bonds. (c) Scalar spin chiralities χ_A and χ_B of the cluster A and B, and their sum $\chi_A + \chi_B$ as functions of D (normalized by the in-plane interaction J_1) obtained by a numerical calculation (see text).

Incorporation of the DM interaction, $\boldsymbol{D}_{ij} \cdot (\boldsymbol{S}_i \times \boldsymbol{S}_j)$, changes the situation dramatically. The DM vectors $\boldsymbol{D}_{ij}$ are locally defined on the bonds connecting two spins, and become finite when the local inversion symmetry is absent. Because of the absence of inversion symmetry on the Fe(i)-Fe(l) bonds, there are finite DM vectors $\boldsymbol{D}_{ij}$ whose directions are illustrated by (yellow) arrows in Fig. 4(b). The DM interaction causes canting of the Fe(l) spins and thus modifies the spin structure. Since the vectors $\boldsymbol{D}_{ij}$ on the upper Fe (i)-Fe(l) bonds are opposite to those on the lower Fe(i)-Fe(l) bonds in each heptamer, the spin canting becomes inequivalent between the basal and top triangle planes, i.e., $\boldsymbol{S}_m \neq \boldsymbol{S}'_m$ and $\tilde{\boldsymbol{S}}_m \neq \tilde{\boldsymbol{S}}'_m$. Moreover the Fe(l) spins cant in a different manner between the clusters A and B. For the Fe(l) triads of the cluster A, directions of the three Fe(l) spins are modified while keeping the original chirality for the case without DM interaction, whereas for those of the cluster B the spin canting alters the chirality value. Owing to the inequivalent modifications of the spin structure, the two contributions χ_A and χ_B no longer cancel out, and the net scalar spin chirality proportional to $\chi_A + \chi_B$ becomes nonzero, which works as an origin of the observed THE.

The above discussion is confirmed by numerical simulations of a classical Heisenberg model on the heptamer spin clusters. In this model, the spins are treated as classical vectors whose norms are set to be unity. The model contains the symmetric exchange interactions, DM interaction, magnetic anisotropy, and Zeeman coupling. For the symmetric exchange interactions, we consider antiferromagnetic $3J_1$ between the in-plane Fe(l)-Fe(l) spin pairs, ferromagnetic $2J_2$ between the out-of-plane Fe(l)-Fe(l) spin pairs, and weak antiferromagnetic J_3 between the Fe(i)-Fe(l) spin pairs [see Fig. 4(b)]. Since the Fe(l) spins in the 120° order direct along the in-plane bonds at $H = 0$, we includes the following anisotropy term, $-A\sum_i[(\boldsymbol{S}_i \cdot \boldsymbol{l})^2 + (\boldsymbol{S}_i \cdot \boldsymbol{m})^2 + (\boldsymbol{S}_i \cdot \boldsymbol{n})^2]$, where $\boldsymbol{l}$ and $\boldsymbol{m}$ are the Bravis vectors of the triangular lattice and $\boldsymbol{n} = \boldsymbol{l} + \boldsymbol{m}$. The Zeeman couping is given by $-H\sum_i S_{zi}$. For the parameter values to simulate the low-T case, we take $J_1 = 1, J_2 = -0.5, J_3 = 0.2, A = 0.2$, and $H = 0.1$. We numerically search the lowest-energy spin configurations, and calculate the scalar spin chiralities χ_A and χ_B as functions of strength of the DM vector $|\boldsymbol{D}_{ij}| = D$ as shown in Fig. 4(c). In the absence of the DM interaction ($D = 0$), χ_A and $-\chi_B$ are equivalent. As D increases, $-\chi_B$

decreases whereas χ_A does not change, which results in finite $\chi_A + \chi_B$. In reality, for D to be effective to generate the spin chirality (empirically, $D/J = 0.1$–0.2), the averaged moment value of Fe(i) spin and the canting angle of the in-plane Fe(l) spin moments by DM interaction are essential; the former is mainly determined by magnetic field, while the latter by D/J. This may explain the low-temperature (30 K) and the nearly H-linear evolutions of THE as observed.

In conclusion, we have investigated the Hall effect in the triangular-lattice $Fe_{1.3}Sb$ under H applied perpendicular to the basal plane. In the relatively-high-T region of the 120° spin-ordered structure on the triangular lattice, the Hall resistivity is negative in sign and well described as composed of the conventional normal and anomalous components. In the low-T region below 30 K, however, the significant positive contribution is observed to be added to the Hall resistivity. This novel term is explained in terms of the scalar spin chirality which originates from the spin modulation by DM interaction in the spin heptamer clusters formed around the respective Fe(i) sites.

We thank S. Miyahara, N. Furukawa, N. Nagaosa, G. Tatara, and Y. Onose for fruitful discussions. This work was in part supported by the Grant-in-Aid for Scientific Research (Grant No. 20340086.) and JSPJ Fellows, and by the Funding Program for World-Leading Innovate R& D on Science and Technology (FIRST program) on ''Quantum Science on Strong Correlation''.

[1] N. Nagaosa *et al.*, Rev. Mod. Phys. **82**, 1539 (2010).
[2] T. Jungwirth, Q. Niu, and A. H. MacDonald, Phys. Rev. Lett. **88**, 207208 (2002).
[3] M. Onoda and N. Nagaosa, J. Phys. Soc. Jpn. **71**, 19 (2002).
[4] R. Karplus and J. M. Luttinger, Phys. Rev. **95**, 1154 (1954).
[5] Y. Yao *et al.*, Phys. Rev. Lett. **92**, 037204 (2004).
[6] Z. Fang *et al.*, Science **302**, 92 (2003).
[7] Y. Taguchi *et al.*, Science **291**, 2573 (2001).
[8] Y. Machida *et al.*, Phys. Rev. Lett. **98**, 057203 (2007).
[9] Even in such a case, the HE induced by the scalar spin chirality may emerge in materials with the crystal structure including inequivalent multiple loops in a unit cell [10–12]. The spin chirality induced HE in pyrochlore magnets correspond to this category.
[10] M. Onoda, G. Tatara, and N. Nagaosa, J. Phys. Soc. Jpn. **73**, 2624 (2004).
[11] K. Ohgushi, S. Murakami, and N. Nagaosa, Phys. Rev. B **62**, R6065 (2000).
[12] R. Shindou and N. Nagaosa, Phys. Rev. Lett. **87**, 116801 (2001).
[13] I. Martin and C. D. Batista, Phys. Rev. Lett. **101**, 156402 (2008).
[14] Y. Akagi and Y. Motome, J. Phys. Soc. Jpn. **79**, 083711 (2010).
[15] H. Takatsu, S. Yonezawa, S. Fujimoto, and Y. Maeno, Phys. Rev. Lett. **105**, 137201 (2010).
[16] R. Kumar *et al.*, Phys. Rev. B **32**, 69 (1985).
[17] T. Yashiro *et al.*, J. Phys. Soc. Jpn. **34**, 58 (1973).
[18] P. Amornpitoksuk, D. Ravot, A. Mauger, and J. C. Tedenac, Phys. Rev. B **77**, 144405 (2008).
[19] P. J. Picone and P. E. Clark, J. Magn. Magn. Mater. **25**, 140 (1981).
[20] This assumption is based on the generic feature of the T-independent *transverse* susceptibility for the antiferromagnetic state with the strong anisotropy.